The 56th Israel Annual Conference on Aerospace Sciences

In partnership with

Faculty of Aerospace Engineering, Technion

Ben Gurion University of the Negev

Civil Aviation Authority of Israel

Directorate of Defense R&D, IMoD

Elbit Systems

IMI Systems

Israel Aerospace Industries

Israel Air Force

Israel Society of Aeronautics & Astronautics

Rafael Advanced Defense Systems

Tel Aviv University

Supported by

Boeing

Gordon Center for Systems Engineering

The PAZY Foundation

Proceedings of the 56th Israel Annual Conference on
Aerospace Sciences, Tel-Aviv & Haifa, Israel
March 9-10, 2016

Model Selection for Radar Registration Errors by Comparison of Radar and ADS-B Data

Dmitrii A. Bedin*
Krasovskii Institute of Mathematics and Mechanics of UrB RAS,
Ekaterinburg, 620990, Russia

The paper is concerned a problem of model selection for systematic radar errors. The statistical study is made that compares measurements of position of an aircraft obtained by surveillance radars with ADS-B (Automatic Dependent Surveillance-Broadcast system) measurements of the same aircraft. The main group of predictors is selected which have significant influence on the range and azimuth measurement biases.

I. Introduction

So far, the radars remain the main source of information about aircraft motion for the Air Traffic Control (ATC) service. Any radar measures the range to the object and the azimuth (the angle between the object line of sight and the north direction). A Primary Surveillance Radar (PSR) obtains measurements by processing radio signals reflected from objects. A Secondary Surveillance Radar (SSR) receives signals from object transponders and has additional information about object altitude. There exists a combined type of radars that mix measurements from PSR and SSR located at one site.

The measurements from radars have errors. It is usual to distinguish random errors that are described well by random values and systematic errors which genesis is not random.

The aim of our work is a study of radar systematic errors and selection of their main dependencies on where and how the observed aircraft moves. Furthermore, we are interested in the point of view of ATC engineers on this problem, i.e., what peculiarities can be found during the work with real data.

For evaluation of the systematic errors, we use Automatic Dependent Surveillance-Broadcast (ADS-B) system measurements as the reference standard. The ADS-B system usually transmits measurements of GPS or GLONASS navigation system receivers from an aircraft.

The real data of the radar and ADS-B systems were given by the “NITA” LLC from S.-Petersburg, Russia.

II. Models of systematic errors

Many authors are interested in the problem of evaluation of radar systematic errors. For example, in paper [1], some algorithms are described based on the Kalman filter for measurements in the real time.

In paper [2], authors describe new advanced TRES (Trajectory Reconstruction and Evaluation Suite) system for evaluation of sensor performance in ATC. This system was

*Researcher, bedin@imm.uran.ru

elaborated for Eurocontrol. To assess radar systematic errors and errors of other types of sensors, it is suggested to process the data on a large time interval in off-line regime. In the author's opinion, the main purpose of correction of systematic errors is the stable work of maneuver detection algorithms. For example, if bias in the measurements is not corrected, it can be interpreted wrong as a maneuver in some situations.

In work [3] of our scientific group, as well as in paper [2], the off-line processing of measurements from a large time interval is considered. The three algorithms for evaluation of systematic errors are presented. Each of them works with its own set of hypotheses about type of systematic errors and their dependencies on aircraft location. One of these algorithms belongs to nonparametric regression and works with a model that describes radar biases as an arbitrary vector fields. This algorithm is similar to the algorithm in work [4]. Other two algorithms relate to parametric statistics and use predetermined function of systematic errors with particular dependencies on aircraft motion characteristics and some unknown parameters.

A model of systematic errors, i.e., the type of functional dependency, is the base of construction of any estimation algorithm. To provide stable work, the model should be suitable for real data that can be met in practice. Linear parametric models allow one to implement the powerful theory of the Gauss-Markov estimates.

The Opportunity Trajectory Reconstruction system in paper [2] for processing the real measurements relies on the algorithm [5] with a linear parametric model of radar and ADS-B systematic errors. The authors cite report [6] where this model is introduced. Let a radar l at the instant t measure the location $x(t,a)$ of an aircraft a, and receive range $r(t,a)$ and azimuth $\alpha(t,a)$. Then the measurements of range $z_r(t,a,l)$ and azimuth $z_\alpha(t,a,l)$ are described by the formulas

$$\begin{aligned} z_r(t,a,l) &= r(t,a) + \Delta_{r0}(l) + r(t,a)c_r(l) + w_r(t,l)\,, \\ z_\alpha(t,a,l) &= \alpha(t,a) + \Delta_{\alpha 0}(l) + \cos\alpha(t,a)\,c_{\cos}(l) + \sin\alpha(t,a)\,c_{\sin}(l) + w_\alpha(t,l)\,. \end{aligned} \tag{1}$$

Here, $w_r(t,l)$, $w_\alpha(t,l)$ are the random errors in range and azimuth; the symbols $\Delta_{r0}(l)$, $\Delta_{\alpha 0}(l)$ denote the constant systematic errors in range and azimuth specific for each radar; the coefficient $c_r(l)$ is connected with a part of the radar systematic error in range that depends on range linearly; the variables $c_{\cos}(l)$, $c_{\sin}(l)$ are the radar eccentricity coefficients.

Additionally, the radar has a time bias $\Delta t(l)$ producing a spatial bias in measurements. Formula for the time bias is $\Delta t(l) = t - t'$ where t is a true instant when a measurement was done and t' is an instant associated with this measurement in the radar data. Note that the value $\Delta t(l)$ is conditioned by delays in the radar devices and in the data transfer channels, therefore, the inequality $\Delta t(l) \leqslant 0$ holds. In the Cartesian coordinate system, the measurement shift vector $\Delta x_t(t,a)$ due to the time bias $\Delta t(l)$ is parallel and proportional to the velocity $v(t,a)$ of the aircraft

$$\Delta x_t(t,a) = v(t,a)\Delta t(l)\,.$$

In the polar coordinate system, the bias $\Delta\, t(l)$ leads to a shift in the range measurement proportional to the range rate $v_r(t,a)$ and to a shift in the azimuth measurement proportional to the angular rate $\omega_\alpha(t,a)$

$$\begin{aligned} \Delta r(t,a) &= v_r(t,a)\Delta t(l)\,, \\ \Delta\alpha(t,a) &= \omega_\alpha(t,a)\Delta t(l)\,. \end{aligned} \tag{2}$$

As we are going to evaluate the radar systematic errors by comparison with ADS-B data, the model of the latter is very important to us. In study [5], the authors mention the time bias as the main source of the ADS-B systematic errors. In this case, the bias value depends on the aircraft: each aircraft a has its own time bias. We shall use the symbol $\Delta t(a)$ to distinguish the dependency on a from the dependency on radar in $\Delta t(l)$.

III. Procedure of comparison of radar and ADS-B measurements. Measurements smoothing and interpolation

Radar and ADS-B measurements are not synchronized in time and sensors receive them at distinct instants. Algorithm of comparison must be able to interpolate the location of an aircraft to some given instant using measurements at other instants. It is more natural to do so for the ADS-B measurements because, on the one hand, this system is more precise and its measurements have smaller random error than radars and, on the other hand, its measurements are more frequent. So, we shall use the ADS-B measurements to interpolate location of an aircraft at instants corresponding to the radar measurements.

Besides interpolation of location to predefined time instants, it is important to estimate other parameters of aircraft motion: velocity, acceleration, altitude. To solve this problem, we use the nonparametric regression technique and approximate locally the ADS-B measurements using spatial motion with constant acceleration.

At first, the ADS-B measurements are converted to the geocentric coordinate system [7] (in this coordinates we shall denote them by symbol $z(\tau, a)$). Then we assess the typical time interval $\delta\tau$ between successive measurement instants into each aircraft trajectory. For this, all ADS-B measurement instants τ_i are sorted in ascending order; then the cumulative density function is constructed for the differences between successive instants. To estimate $\delta\tau$, we take the median of this "distribution".

Let t be a time instant for interpolation. Consider all ADS-B measurements with time instants in the interval $[t - k\delta\tau, t + k\delta\tau]$ (appropriate k is chosen preliminary, $k = 4$ or 5 is usually suitable). In the work, we fit locally these measurements using the following simple model of the aircraft motion:

$$z(\tau, a) = x_0(t) + v_0(t)\,(\tau - t) + a_0(t)\,(\tau - t)^2 + w_{\text{ads}}(\tau)\,. \tag{3}$$

Here, $x_0(t)$, $v_0(t)$, $a_0(t)$ are the vector parameters of the aircraft motion at the instant t: the location, velocity, and acceleration in the geocentric coordinate system; the symbol $w_{\text{ads}}(\tau)$ denotes the error of the ADS-B measurement. The fit is built by the least squares method.

In next stage, the estimate $x_0(t)$ of the aircraft location is translated to the polar coordinate system of radar, and we calculate the differences in range $dr(t)$ and azimuth $d\alpha(t)$ between the radar measurement and our estimate (a "smoothed" ADS-B measurement). This procedure is applied independently to any radar measurement. As a result, for any radar measurement at an instant t, a data set is produced wherein the differences $dr(t)$, $d\alpha(t)$, the estimates for aircraft location $x_0(t)$, its range, azimuth, velocity $v_0(t)$, acceleration, altitude, elevation angle, and others values that characterize the motion are located.

The further objects of research are differences dr and $d\alpha$. Write for them a full model proposed in [5]. For this, include in formula (1) the time bias term for the radar data by formula (2) with the positive sign and the time bias term for the ADS-B data by the same formula with the negative sign

$$dr(t,a,l) = \Delta_{r0}(l) + r(t,a)c_r(l) + v_r\left(\Delta t(l) - \Delta t(a)\right) + w_r(t,l)\,, \tag{4}$$
$$d\alpha(t,a,l) = \Delta_{\alpha 0}(l) + \cos\alpha(t,a)\,c_{\cos}(l) + \sin\alpha(t,a)\,c_{\sin}(l) + \omega_\alpha\left(\Delta t(l) - \Delta t(a)\right) + w_\alpha(t,l)\,.$$

Note that $\Delta t(l)$ is the time bias for radar l and $\Delta t(a)$ is the time bias for the ADS-B connected with particular aircraft a.

IV. Analysis of differences between radar and ADS-B measurements

For the study, the data from the Moscow ATC zone are used. The data have been received from the surveillance radars and the ADS-B system servers. The total duration of the entire record is one day. The data are divided into separate tracks for distinct aircrafts by means of the program for multiradar surveillance provided by the "NITA" company. The total number of tracks taken for the further studies is 765.

Each trajectory is processed by means of the local approximation algorithm. As a result, for radars and ADS-B measurements, the differences $dr(t)$, $d\alpha(t)$ are formed with additional records including such characteristics of the aircraft motion as the time instant t, the range r, the azimuth α, the altitude h, the elevation angle β (show the elevation of the line of sight above the horizon), the radial v_r and angular ω_α rates, the quality indicator for the ADS-B information, and the geographic coordinates of the aircraft.

The calculated differences are analyzed to find out dependencies on characteristics mentioned above. The primary analysis is implemented visually. The following conclusions have been made:

1. There is no any noticeable statistical dependency between the differences in range dr and in azimuth $d\alpha$. The main hypothesis is the absence of the correlation between them and, consequently, between random errors in range and azimuth for both information sources: radar and ADS-B.

2. There is no any clear dependency of differences in range dr and azimuth $d\alpha$ on the altitude h and elevation angle β.

3. The differences dr in range strongly depend on the range r and the radial rate v_r of the aircraft motion. A clear dependency on the azimuth α or the angular rate ω_α is not found out, as well as, any correlation with other characteristics of the aircraft motion.

4. The dependency of dr on the radial rate v_r is close to linear and differ for distinct aircraft trajectories: any trajectory has its own coefficient of the slope.

5. The dependency of dr on the range r is very close to linear and the coefficient of the slope seems to be the same for all radars of all radar types: primary, secondary, and combined.

6. The level of the random noise in the range measurements seems to be significantly different for distinct aircraft trajectories.

7. The differences in azimuth $d\alpha$ have a weak dependency on the range r. At distances less than 320 km, the slope is small, and we can say about the approximately "flat" or constant systematic error in azimuth. However, for some radars, there is a sharp

change of the slope at distances about 320 km. But for distances greater than 320 km, these radars show the dependency of $d\alpha$ on range r that looks like linear with a large slope coefficient. Other radars demonstrate a "flat" type of slope everywhere.

8. There are some radars with dependency of $d\alpha$ on azimuth α. The character of such a dependency does not always look like sine function as in model (4). For some radars, there exist large deviations from this shape.

9. For many radars (the number of them is about a half of the total number of radars in the Moscow ATC zone), the dependency of $d\alpha$ on azimuth α is absent or negligible.

10. In most cases, if the few radars with different type (primary, secondary, and combined radars) are situated at the one site and, maybe, have common devices, then their differences in azimuth $d\alpha$ have similar values and almost coincide in the common area. However, there exist some radars situated at one site which behave in other manner and have significantly different levels of differences $d\alpha$ in azimuth. The primary (PSR) and combined radar types can be unified in one group according to the fact that there are no significant differences between their levels of $d\alpha$. The large differences of levels can be between secondary (SSR) and primary (or combined) radars only.

11. For the differences in range dr, we have not found any clear diversity among radar with different types situated at one site.

12. The total pattern of measurements are constant in time. However, some jump-like changes in time of differences dr, $d\alpha$ have been noticed. These events seem to be connected to device kit switches in corresponding radars.

13. There is a small number of radars with periodical perturbation in dr. For these radars, the same perturbation for value $rd\alpha$ is noticeable for small distances r with the $\frac{\pi}{2}$ azimuth offset with respect to the perturbation in dr. It has been found out that the reason of such an effect is incorrect radar coordinates used for evaluation. This type of error can be easily fixed and these perturbations have been removed from the data.

In Figures 1–3, a typical pattern for dependency of the range differences dr on the range r and the radial rate v_r is shown. All measurements are received from radars at one site in Moscow ATC zone. Refer this site as site 1. The differences dr for SSR have blue color. Red color marks the measurements of combined radar. The pattern of measurements in the figures gives us a supposition that the systematic and random errors for both radars have equal characteristics. There is no any discontinuity in the data at the point where the SSR measurements end and the combined measurements begin.

Figure 1 shows dependency of dr on the range r. The affine type of the dependency is clearly shown: the graph looks like it has an intercept with the dr axis at some level and linear growth in r. There are additional "clouds" of measurements above and below the graph. They go parallel to the main trend line. Figure 2 shows a graph of the dependency of dr on the radial rate v_r and explains the phenomenon of additional "clouds" in the previous figure. It is shown that there are measurements with different "reaction" on the same v_r level. The "cross" in the middle of the figure consists of measurements of two distinct trajectories: each trajectory has different slope of the graph with respect to v_r.

The first trajectory has the slope which is approximately equal to zero but the second one has a positive trend with additional 200 m in dr for every 100 m/s in radial rate. More detailed analysis shows that other trajectories have the same peculiarity and the deviations in dr at large positive and negative levels of v_r can be explained by this.

Based on Fig. 2, it seems to be true that at zero v_r there is no divergence in the dr value. Figure 3 confirms this hypothesis. This figure shows three-dimensional graph of the dependency of dr on r and v_r. The point of view is taken near small v_r values, so, we can see the "cloud" of measurement along the trend line parallel to the r axis. We see that the bundle of measurements narrows linearly toward to a point (this point is different for distinct r) when v_r tends to 0. In Figure 4, this three-dimensional graph is shown from another point of view.

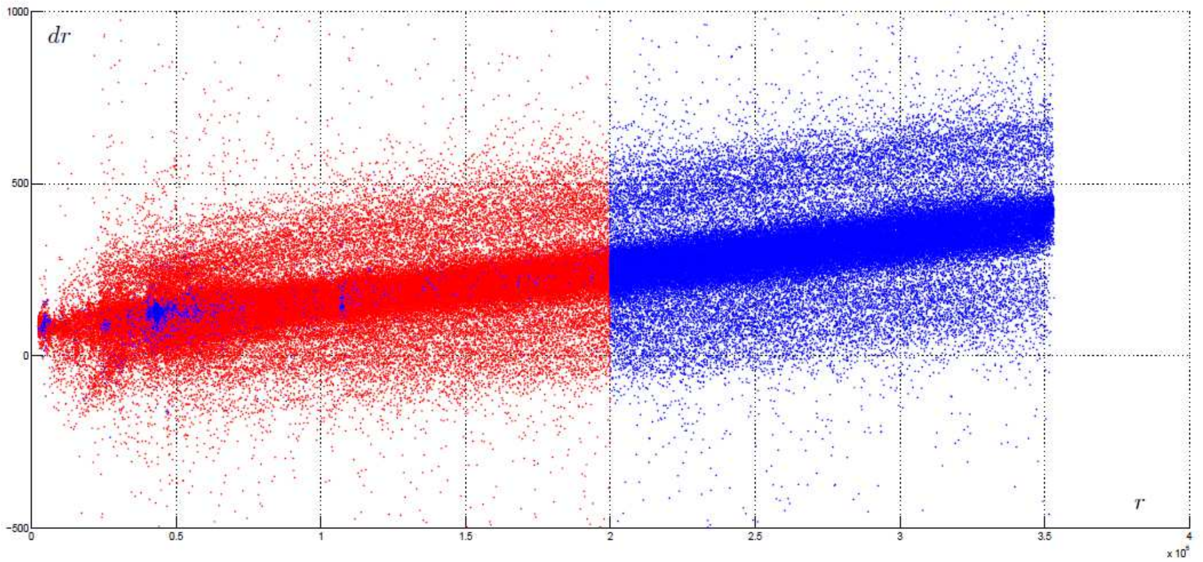

Figure 1. The dependency of dr on the range r for radars at the site 1 in Moscow ATC zone. The measurements of SSR are blue, the measurements of the combined radar are red. The values of dr and r are specified in m

In Figure 5, the graph of dependency of $d\alpha$ on the range r is shown for the same radars at the site 1 in Moscow ATC zone. In this figure, colors of dots mean the same as for graphs for dr: the blue color is connected with the SSR measurements and the red color is for measurements of the combined radar. The pattern of the measurements is quite typical: the figure depicts the most peculiarities in the azimuth measurements for all radars. Figure 5 confirms that the measurements of both SSR and combined radars have approximately a constant (flat) type of dependency of the systematic errors in the azimuth on the range r. For the site 1, almost all measurements in distances up to 200 km belong to combined radar; in farther distances, the measurements are received by SSR only. We see the jump in the level of $d\alpha$ at the point where the measurements of the combined radar change to the SSR measurements near 200 km. However, measurements of both SSR and combined radars look flat if we consider them separately for distances about 200 km and closer. But at distance 320 km, the SSR measurements change their character: it is noticeable in the figure that the differences in $d\alpha$ have almost linear growth farther than 320 km and the slope is approximately 0.8 degree per 100 km.

The radars at site 1 do not show clearly the dependency of $d\alpha$ on α. This feature is proved by Fig. 6. But it does not to be so for other radars. Figures 7, 8 show the

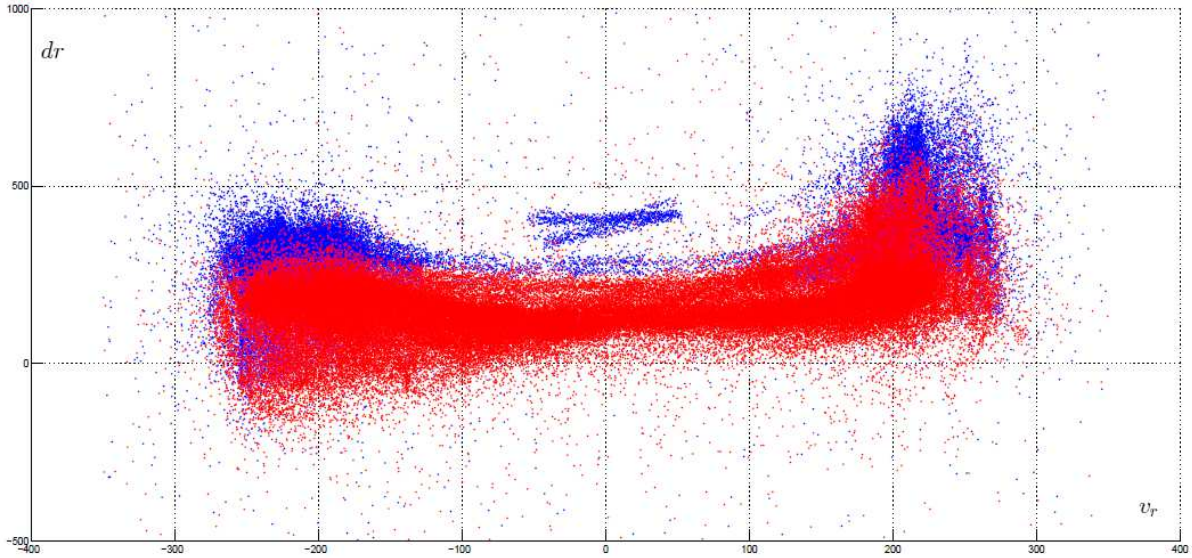

Figure 2. The graph of the dependency of dr on v_r for the radars at the site 1. The values of dr are specified in m, v_r are specified in m/s

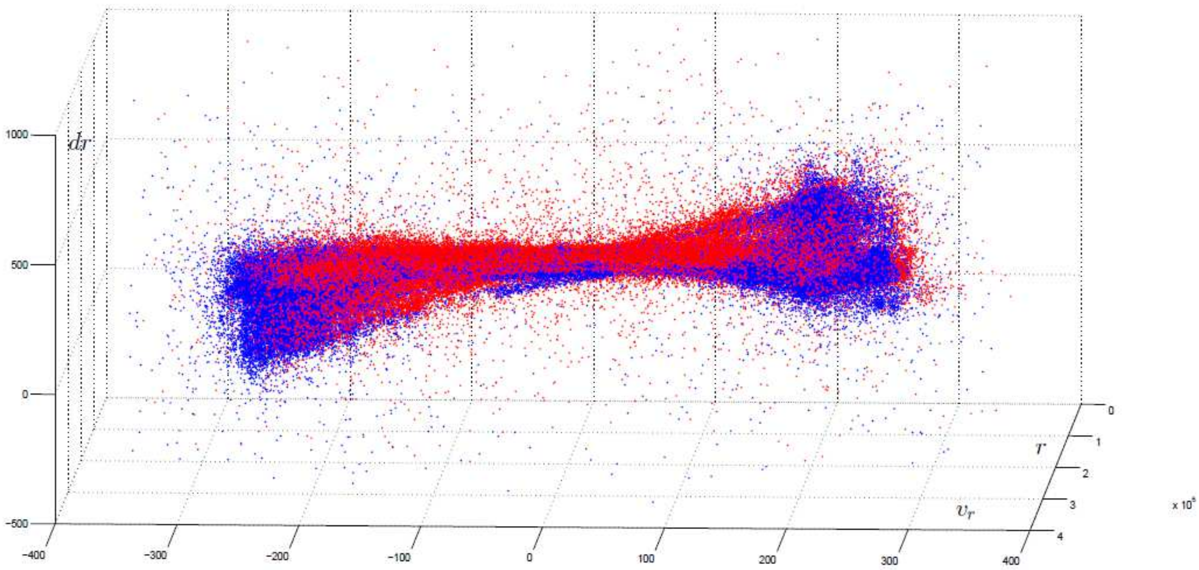

Figure 3. A three-dimensional graph of the dependency of dr on v_r and v_r for the radars at the site 1. The linear connection of the v_r level and divergence in dr is clearly visible. The values of dr and r are specified in m, v_r are specified in m/s

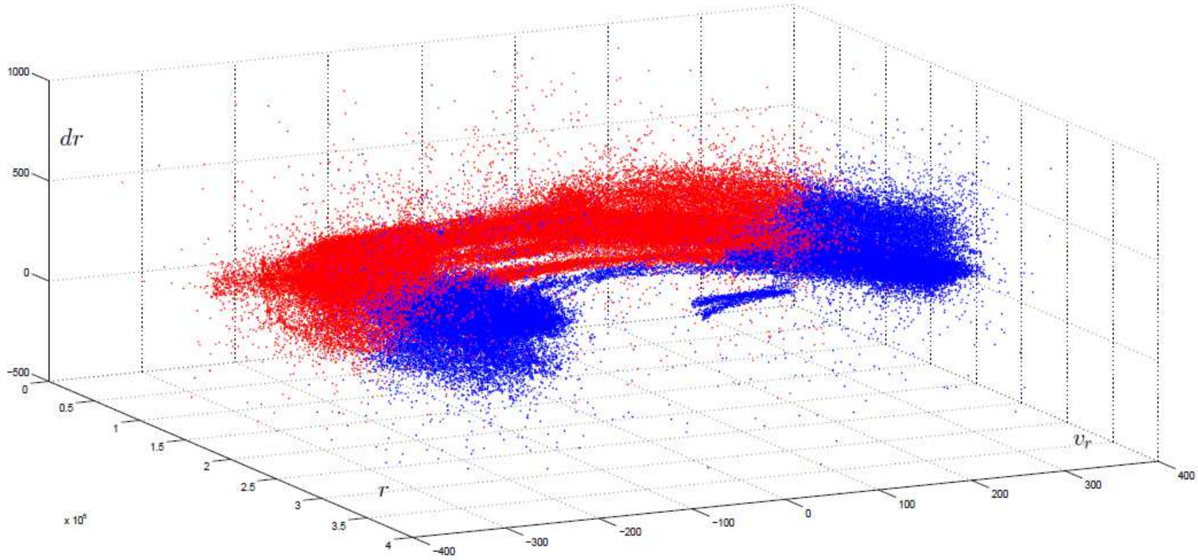

Figure 4. The same three-dimensional graph of the dependency of dr on v_r and v_r for the radars at the site 1 from other point of view. The values of dr and r are specified in m, v_r are specified in m/s

dependencies of the differences in azimuth $d\alpha$ on azimuth α for the PSR and SSR that are placed both at other location site in Moscow ATC zone. Further, we shall use the name "site 2" for it. The green color denotes the PSR measurements and blue color is used for the SSR measurements as in the previous figures. There is a significant discrepancy between behavior of these two radars. Both graphs show a complicated pattern of the dependency on α. The function $f(\alpha, l)$ for PSR resembles a misshaped sine function (Fig. 7). But the function for SSR is much more complicated and looks like a sawtooth (Fig. 8).

The complicated variants of the dependency for radar azimuth measurements on azimuth are mentioned in literature earlier. In technical report [8] of the Intersoft Electronics NV company, it was pointed out that the radome (special cover for radar) can be source of such a distortion. The other important source of systematic errors is lightning rods and another objects that are placed near the radar. The third source is azimuth change pulse glitches in the system of surveillance on antenna rotation.

Taking into account the visual analysis, we can suggest a new model for the dependencies of the radar errors. This model is more complicated than model (4)

$$\begin{aligned} dr(t,a,l) &= \Delta_{r0}(l) + r(t,a)c_r(l) + v_r\left(\Delta t(l) - \Delta t(a)\right) + w_r(t,l)\,, \\ d\alpha(t,a,l) &= L(r, \Delta_{\alpha 0}(l), \Delta_{\alpha 320}(l), \Delta_{\alpha 400}(l)) + f(\alpha, l) + \omega_\alpha\left(\Delta t(l) - \Delta t(a)\right) + w_\alpha(t,l)\,. \end{aligned} \tag{5}$$

Here, L is the function

$$L(r) = \begin{cases} (1-c)\Delta_{\alpha 0} + c\Delta_{\alpha 320}\,, & r \in [0, 320]\,, \quad c = \frac{r}{320}\,, \\ (1-c)\Delta_{\alpha 320} + c\Delta_{\alpha 400}\,, & r > 320\,, \qquad c = \frac{r-320}{400-320}\,, \end{cases}$$

for the range r specified in km; the constants $\Delta_{\alpha 320}$, $\Delta_{\alpha 400}$ (and $\Delta_{\alpha 0}$, too) denote levels of the systematic error in azimuth at distances 320, 400 (and 0) km; the symbol $f(\alpha, l)$ denotes a term for dependency of $d\alpha$ on azimuth α. As it mentioned above, $f(\alpha, l)$ can be an arbitrary continuous function, but it is approximately equal to zero for most radars.

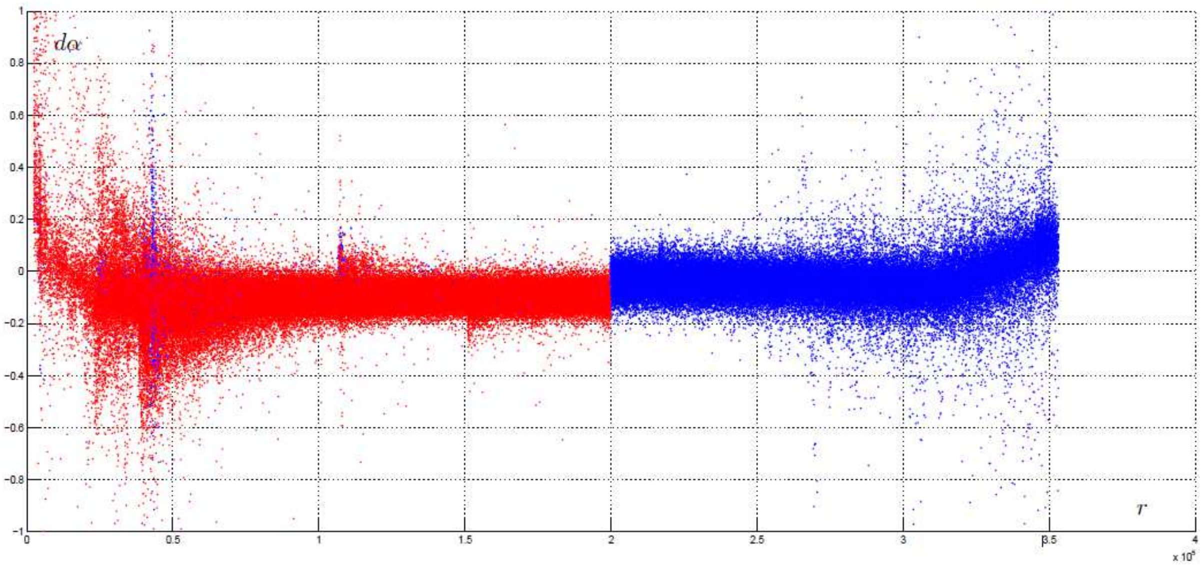

Figure 5. The graph of the dependency of $d\alpha$ on range r for the radars at the site 1 in Moscow ATC zone. The measurements of SSR are blue, the measurements of the combined radar are red. The values of $d\alpha$ are specified in degrees and r are specified in m

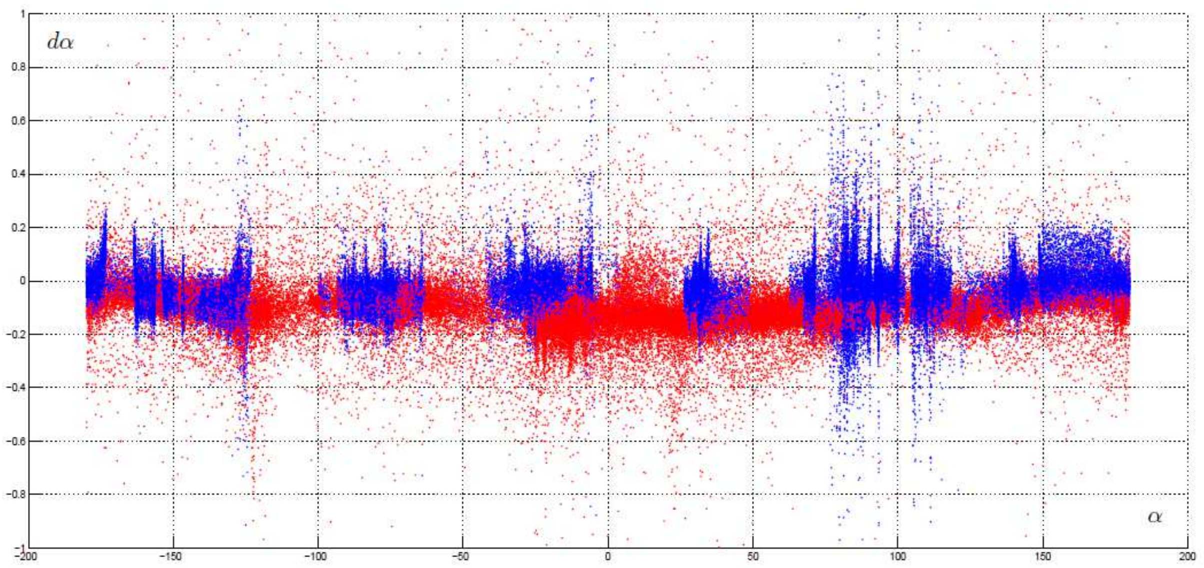

Figure 6. The graph of the dependency of $d\alpha$ on α for the site 1. The values of $d\alpha$ and α are specified in degrees

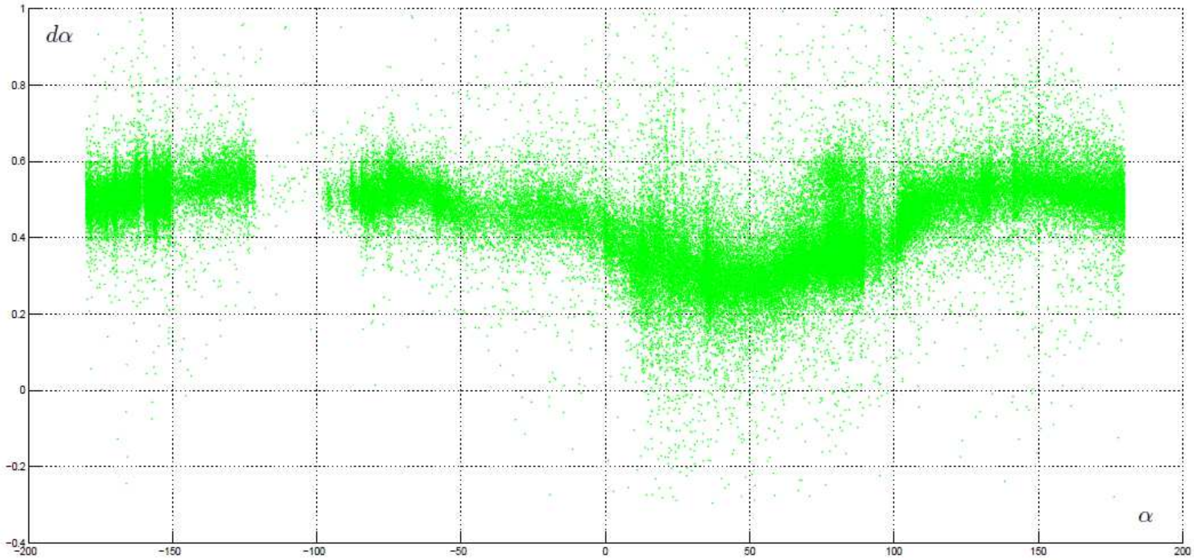

Figure 7. The graph of the dependency of $d\alpha$ on α for PSR at the site 2. The values of $d\alpha$ and α are specified in degrees

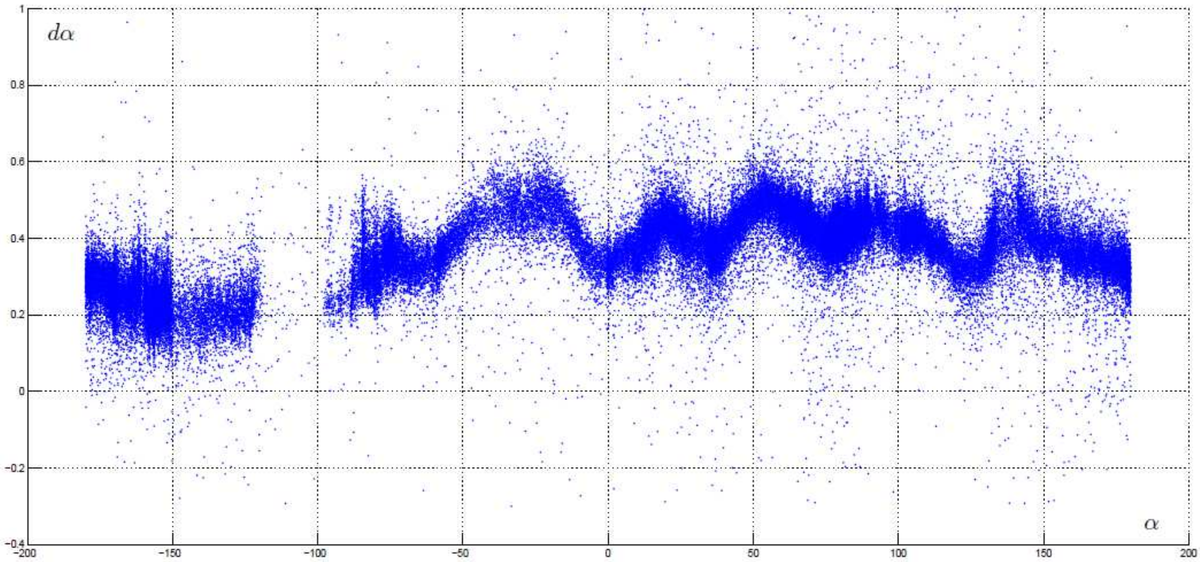

Figure 8. The graph of the dependency of $d\alpha$ on α for SSR at the site 2. The values of $d\alpha$ and α are specified in degrees

It should be noted that the dependency of the differences dr on v_r mentioned in item 5 in the list above can be conditioned not only by means of the time bias $\Delta t(a)$ of the ADS-B data. We cannot exclude other reasons for this behavior, for example, disparity in quality of aircraft transponders or peculiarities in radar devices and software. The coefficient of the linear dependency of dr on v_r can differ not only for distinct trajectories but for distinct radars also. For this reason, we should consider a more complicated model than model (5)

$$\begin{aligned} dr(t,a,l) &= \Delta_{r0}(l) + r(t,a)c_r(l) + v_r \Delta t(l,a) + w_r(t,l)\,, \\ d\alpha(t,a,l) &= L(r, \Delta_{\alpha 0}(l), \Delta_{\alpha 320}(l), \Delta_{\alpha 400}(l)) + f(a,l) + \omega_\alpha \Delta t(l,a) + w_\alpha(t,l)\,. \end{aligned} \tag{6}$$

Here, the coefficient $\Delta t(l,a)$ of the time bias depends on both radar and aircraft.

The comparison of these three models (4), (5), and (6) has been taken for real data. Models (5), (6) are tested with function $f(\alpha,l) = \cos\alpha(t,a)\, c_{\cos}(l) + \sin\alpha(t,a)\, c_{\sin}(l)$ that completely coincides with the eccentricity function in model (4). We refuse to use of an arbitrary continuous function $f(\alpha,l)$ because it requires much more sophisticated methods of the semiparametric statistics.

The whole data are divided into a training set and a test set. Sizes of the sets are 0.7 and 0.3 of the whole data set, respectively. A 10-fold cross-validation is applied to the training set for comparison the models. Then all models are applied to the whole training set, and the result of the learning process is applied to the test set to assess a performance finally.

The learning method is fit. We use weighted mean squared error as the loss function for learning

$$J = \frac{1}{\hat\sigma_r^2} \sum_i (dr_i - d\hat{r}_i)^2 + \frac{1}{\hat\sigma_\alpha^2} \sum_i (d\alpha_i - d\hat\alpha_i)^2 \,.$$

In this formula, i is the index for all measurement differences dr, $d\alpha$; the symbols $d\hat{r}_i$, $d\hat\alpha_i$ denotes model predictions of values dr, $d\alpha$ at the same points of input variables as for dr_i, $d\alpha_i$. The symbols $\hat\sigma_r$, $\hat\sigma_\alpha$ denotes estimates of mean squared errors for random errors (distortions) in the range and azimuth measurements.

These estimates are based on local approximation (3) applied to radar measurements: the measurements in a short sliding window are fitted by motion with constant acceleration. Then the covariation matrix is estimated by the formula

$$R = \frac{1}{n-3} \sum_{i=1}^{n} (z(\tau_i) - \hat{x_0}(\tau_i))\,(z(\tau_i) - \hat{x_0}(\tau_i))^{\mathrm{T}} \,.$$

Here, 3 is the number of parameters in model (3) of motion with a constant acceleration; n is the number of measurements in window. The mean squared errors of measurements in azimuth $\breve\sigma_\alpha$ and range $\breve\sigma_r$ for this window are taken from the matrix R. Using the whole set of estimates $\{\breve\sigma_r\}$, $\{\breve\sigma_\alpha\}$ for all windows, we choose their medians as $\hat\sigma_r$, $\hat\sigma_\alpha$. Median estimates reflect the typical level of deviations for any small motion segment, in which range, azimuth, and other motion parameters cannot vary a lot. Hence, these estimates reflect mostly just the random noise errors. For the data under consideration, the value of $\hat\sigma_r$ is about 15 m, and the value of $\hat\sigma_\alpha$ is close to $0.025°$.

In the model comparison, the approximation performance is assessed by the residual mean squared (RMS) deviation separately in range and azimuth

$$J_r = \frac{1}{\hat\sigma_r^2} \sum_i (dr_i - d\hat{r}_i)^2 \,, \quad J_\alpha = \frac{1}{\hat\sigma_\alpha^2} \sum_i (d\alpha_i - d\hat\alpha_i)^2 \,.$$

It is established that all three models have approximately equal RMS levels. The RMS level in range is about 100 m and the RMS level in azimuth is approximately 0.1°.

In azimuth, two new models (5) and (6) are slightly more efficient because of the L function effect, but this advantage is not essential. It can be explained by the fact that, in the Moscow ATC zone, only two radars have a significant change of the slope for $d\alpha$ at distances about 320 km.

Model (6) differs from models (5) and (4) since it takes into account the time biases Δt depending on both radar and aircraft. The fact that model (6) has no significant advantage in RMS against (5) and (4) means that the time biases are divided to their sources: there are distinct time bias for aircraft $\Delta t(a)$ and time bias $\Delta t(l)$ for radar. The first of them seems to be provided by ADS-B system.

Models (5) and (6) provide a slightly lower RMS level than model (4). But, on the other hand, model (5) and, especially, model (6) are more complicated and use more variables than (4). Therefore, model (4) is preferred for practical usage if the number of radars with a change of the slope for $d\alpha$ is very small. If there exist many radars of such a type, model (5) can be more useful then (4). Model (6) is too much complicated and not useful.

Notice that the RMS levels for any model are higher than the median levels $\hat{\sigma}_r$, $\hat{\sigma}_\alpha$ of local deviations from the real measurements. It must be admitted that the fit is insufficiently accurate for all models. It seems that the causes of this are an effect of complicated systematic error in azimuth ("tricky" type of the function $f(\alpha, l)$) and "bad trajectories" with jumps and outliers in the range differences dr.

V. Conclusion

A study of radar measurements has been implemented in order to select a suitable model for radar systematic errors. Three variants (4), (5), and (6) of the model of differences between radar and ADS-B measurements have been compared. It is found out that all three models have an approximately equal level of the residual mean squared error: 100 m in range and 0.1° in azimuth. Model (4) is the simplest one. Since the quality of fit is not significantly differ among the models, model (4) is preferred to use if the number of radars with a change of the slope for $d\alpha$ is very small. If it is not so, the model (5) would be the best choice.

Notice that the RMS level for all models is more than the mean squared error for random noise, which is estimated as 15 m in range and 0.025° in azimuth. The draw-back of the approximation quality seems to be connected with a complicated function of dependency of the systematic errors in azimuth on azimuth and presence of outliers in range measurements.

The dependency of the differences dr between radar and ADS-B measurements on v_r can be explained by the ADS-B time biases.

Acknowledgments

The work was supported by Integrated Program of UrB RAS (project No. 15-16-1-13) and by RFBR, research project No. 15-01-07909 a.

References

[1] Taghavi, E., Tharmarasa, R., Kirubarajan, T., and Bar-Shalom, Y., "Bias estimation for practical distributed multiradar-multitarget tracking systems," *Information Fusion (FUSION), 2013 16th International Conference on*, July 2013, pp. 1304–1311.

[2] Besada, J., Soto, A., de Miguel, G., Garcia, J., and Voet, E., "ATC trajectory reconstruction for automated evaluation of sensor and tracker performance," *Aerospace and Electronic Systems Magazine, IEEE*, Vol. 28, No. 2, Feb 2013, pp. 4–17.

[3] Bedin, D., Fedotov, A., Ivanov, A., Patsko, V., and Ganebniy, S., "Coprocessing of data from several radars for determination of systematic errors in azimuth and range," *55th Israel Annual Conference on Aerospace Sciences 2015*, Vol. 2, Technion Israel Institute of Technology, 2015, pp. 1320–1334.

[4] Karniely, H. and Siegelmann, H., "Sensor registration using neural networks," *Aerospace and Electronic Systems, IEEE Transactions on*, Vol. 36, No. 1, Jan 2000, pp. 85–101.

[5] Besada, J., de Miguel, G., Tarrio, P., Bernardos, A., and Garcia, J., "Bias estimation for evaluation of ATC surveillance systems," *Information Fusion, 2009. FUSION '09. 12th International Conference on*, IEEE, 2009, pp. 2020 – 2027.

[6] Fischer, W. L., Cameron, A. G., and Muehe, C., "Registration Errors in a Netted Air Surveillance System," Technical Note 40, MIT Lincoln Laboratory, Lexington, MA, 1980.

[7] Torge, W., *Geodesy*, Berlin, Germany: Walter de Gruyter, 3rd ed., 2001.

[8] Pchelintsev, A., "Radar Alignment and Accuracy Tool: RASS-R Radar Comparator Dual," Electronic report, Intersoft Electronics NV, http://www.intersoft-electronics.com/Downloads/Publications, August 2009.